

A Multifunctional LNA Oligonucleotide-Based Strategy Blocks AR Expression and Transactivation Activity in PCa Cells

Daniela Castanotto,^{1,9} Xiaowei Zhang,^{1,9} Jacqueline Rüger,¹ Jessica Alluin,² Ritin Sharma,³ Patrick Pirrotte,³ Lars Joenson,⁴ Silvia Ioannou,⁵ Michael S. Nelson,⁶ Jonas Vikeså,⁴ Bo Rode Hansen,⁷ Troels Koch,⁸ Mads Aaboe Jensen,⁴ John J. Rossi,² and Cy A. Stein¹

¹Department of Medical Oncology, City of Hope, 1500 East Duarte Road, Duarte, CA 91010, USA; ²Department of Molecular and Cellular Biology, City of Hope, 1500 East Duarte Road, Duarte, CA 91010, USA; ³Collaborative Center for Translational Mass Spectrometry, Translational Genomics Research Institute, Phoenix, AZ, USA; ⁴Roche Innovation Center Copenhagen A/S, Fremtidsvej 3, 2970 Hørsholm, Denmark; ⁵Science Department, Flintridge Preparatory School, 4543 Crown Avenue, La Cañada Flintridge, CA 91011, USA; ⁶The Light Microscopy and Digital Imaging Core, Beckman Research Institute, City of Hope, 1500 East Duarte Road, Duarte CA 91010; ⁷Genevant Sciences, 245 Main Street, Floor 2, Cambridge, MA 02142; ⁸Frederikskaj 10B, 2nd floor, 2450 Copenhagen SV, Denmark

The androgen receptor (AR) plays a critical role in the development of prostate cancer (PCa) through the activation of androgen-induced cellular proliferation genes. Thus, blocking AR-mediated transcriptional activation is expected to inhibit the growth and spread of PCa. Using tailor-made splice-switching locked nucleic acid (LNA) oligonucleotides (SSOs), we successfully redirected splicing of the AR precursor (pre-)mRNA and destabilized the transcripts via the introduction of premature stop codons. Furthermore, the SSOs simultaneously favored production of the AR45 mRNA in lieu of the full-length AR. AR45 is an AR isoform that can attenuate the activity of both full-length and oncogenic forms of AR by binding to their common N-terminal domain (NTD), thereby blocking their transactivation potential. A large screen was subsequently used to identify individual SSOs that could best perform this dual function. The selected SSOs powerfully silence AR expression and modulate the expression of AR-responsive cellular genes. This bi-functional strategy that uses a single therapeutic molecule can be the basis for novel PCa treatments. It might also be customized to other types of therapies that require the silencing of one gene and the simultaneous expression of a different isoform.

INTRODUCTION

Prostate cancer (PCa) is the second most common cancer in men worldwide.¹ In the United States, approximately 190,000 new PCa cases will be diagnosed in 2020.² Of these, an estimated 30,000 cases will end in death, making PCa the second most deadly cancer in men.² The most important molecular driver in PCa is the androgen receptor (AR).^{3–5} The AR, found in the cytoplasm, responds to androgen signaling by translocating to the cell nucleus where it acts as a regulator of gene transcription.⁶ The AR is a key evolutionary gene that plays a critical role in male sexual development and in the maintenance of the male phenotype throughout life. Hence, it is to be expected that cells have evolved ways to maintain AR function.

The full-length AR (AR-FL) precursor (pre-)mRNA generally consists of eight exons (Exs). Exons 5–8 encode the ligand-binding domain (LBD) (i.e., the testosterone/dihydrotestosterone [DHT] binding site). Under selective pressure from some of the anti-androgenic drugs administered to patients, the AR can undergo mutations that enable expression of shorter oncogenic forms. These oncogenic AR isoforms, including those lacking the LBD, remain active and can function in place of the AR-FL. A common strategy, blocking the AR transactivation function in later stage PCa, is known as androgen deprivation therapy (ADT). This form of treatment relies on the use of drugs that block the binding of androgens to the LBD of the AR protein, which inhibits its translocation from the cytoplasm to the nucleus. At the outset, ADT generally results in tumor regression, but, as mentioned above, hormone-independent AR isoforms can later surface and lead to castration-resistant PCa (CRPC).^{7–10} These CRPC-driving AR isoforms lack the LBD of the AR that is encoded by the C-terminal exons of the AR pre-mRNA.¹¹ The most common CRPC-related AR isoform is ARv7, present in 20%–40% of patients who previously underwent ADT.¹² In the ARv7 mRNA, exons 4–8, which include the DNA-binding domain, are spliced out.¹³ Therefore, those agents used for PCa therapy, e.g., enzalutamide (Xtandi), which bind to the LBD, are ineffective.¹² Newer generations of non-steroidal anti-androgens such as apalutamide (Erleada)¹⁴ and darolutamide (Nubeqa),¹⁵ which were US Food and Drug Administration (FDA) approved in 2018 and 2019,

Received 11 August 2020; accepted 21 October 2020;
<https://doi.org/10.1016/j.omtn.2020.10.032>.

⁹These authors contributed equally

Correspondence: Daniela Castanotto, Department of Medical Oncology, City of Hope, 1500 East Duarte Road, Duarte, CA 91010, USA.

E-mail: dcastanotto@coh.org

Correspondence: Cy A. Stein, Department of Medical Oncology, City of Hope, 1500 East Duarte Road, Duarte, CA 91010, USA.

E-mail: cyastein@gmail.com



respectively,^{16,17} improve metastasis-free survival of CRPC patients. However, they have significant toxicity and do not provide a long-term, permanent solution.¹⁸

Although nearly all AR variants translocate to the nucleus and transactivate survival genes, one alternatively spliced isoform, AR45,¹⁹ does not exhibit this oncogenic activity. AR45 contains the DNA-binding domain and LBD, but it lacks AF-1, the transactivating N-terminal domain (NTD) encoded in the first exon of the AR transcript. This is important because the AR activation function relies primarily on this first activation domain within the N-terminal region (NTR),²⁰ which contains transcriptional activation units 1 and 5 (TAU-1 and TAU-5). TAU-1 makes up almost the entire transactivation domain and is required to activate the AR-FL protein.²¹ TAU-5 is a smaller region that is required and sufficient to activate AR isoforms that lack the LBD.²¹ TAU-1 and TAU-5 are therefore necessary for AR transcriptional activity.^{22,23} This explains why AR spliced isoforms that lack the second transactivation domain (AF-2) and the LBD²¹ (e.g., ARv7) can maintain potent transactivation properties. The AR NTD has little homology with other steroid receptors and is the least conserved of all AR domains; consequently, the NTD is difficult to target with small molecular therapeutic entities. As long as this NTD region is present and functional, the AR and all of its isoforms will continue to transactivate nuclear genes and promote tumor cell survival.

In this study, we performed a splice-switching oligonucleotide (SSO)²⁴ screen to identify sequences that best drove production of AR proteins from the AR-FL and its derived isoforms toward AR45. To alter the splicing pattern, we used 16- to 20-mer phosphorothioate (PS) SSOs, each containing six to eight interspersed locked nucleic acid (LNA) moieties,²⁵ and targeted them either at, upstream, or downstream of the 3' or 5' splice sites of the AR-FL. Binding sites for the SSOs on the AR transcripts were chosen based on which SSO caused the most effective re-direction of splicing to selected alternative cryptic splice sites, and destabilized the resulting transcripts by triggering nonsense-mediated decay (NMD).²⁶ Preference was given to those SSOs that could also favor the production of the AR45 mRNA in lieu of the AR-FL mRNA. Using this strategy, we identified powerful SSOs that silenced AR expression and modulated the expression of AR-responsive genes. Our "multitask" design SSO could be the basis for more effective PCa treatments, especially for patients with CRPC.

RESULTS

Suppression of AR Gene Expression via an NMD Pathway

When the selective pressure from anti-androgenic drugs given to patients leads to the expression of truncated AR isoforms, it is difficult to specifically block their oncogenic activity with small molecules. This is because these short isoforms do not include the LBD, the targeted region of small molecule-based drugs. Therefore, we focused on developing a strategy that would be unaffected by the absence of the LBD. Strategies targeting the spliceosome have been used to alter AR-FL alternative splicing and to block production of these short isoforms.²⁷ However, the spliceosome is not specific to a single gene, so

this approach may produce unacceptable cellular toxicity. Several antisense oligonucleotides (ASOs) targeting the AR have also been used with promising results, including one that is currently in a phase I clinical trial.^{28,29} Nonetheless, the analysis of 914 samples from five independent studies indicated that both RNaseH2A and RNaseH2B are depleted in PCa.³⁰ Downregulation of RNaseH2B, which is required for ASO activity, could present a significant challenge to the use of ASOs.

When fully chemically modified, SSOs are highly stable *in vivo* and may in fact be preferred for therapeutic purposes. Indeed, such chemical entities (e.g., eteplirsen) have demonstrated efficacy in clinical trials and have been FDA approved and commercialized.^{24,31} We designed the SSO-based strategy reported herein based on the assumption that if silencing takes advantage of a natural cellular process, it might be better tolerated by cells and more long-lasting. We therefore targeted the SSOs to canonical splice sites in the AR pre-mRNA transcript to block and/or redirect the splicing in a manner that would result in the inclusion of premature termination codons (PTCs). The introduction of PTCs upstream of an exon-exon junction triggers NMD, which leads to translational repression and degradation of the mRNA.³² We performed proof-of-principle experiments using sequences encompassing either the 5' splice site (ss), the 3' ss, or the polypyrimidine tract, an intronic splicing regulatory sequence (Figure 1; Figure S1). We specifically targeted the first intron of the AR with the goal of eliminating the NTD encoded by exon 1. As mentioned above, the NTD domain can, in the absence of the remainder of the protein, function as a transcription activator. Therefore, any splicing alteration in the downstream introns/exons might generate new, stable isoforms with transactivation activity. The NTD is common to *all* AR variants (except for AR45), extending the targeting potential of our SSOs.

The first SSO targeting the canonical 3' ss of intron 1 (SSO753, Figures 1A and 1B; Figures S1A and S1B) also spanned and blocked an adjacent 3' ss. This latter site, if utilized as an alternative splice site, would create a translatable open reading frame (ORF). SSO753 was also designed to base-pair almost entirely with exon 2 and to block only a single nucleotide (G) of the 3' ss AG. Our intent here was to generate an SSO with a dual function. These functions are (1) to arrest the splicing at the canonical AG (the proximal SSO/pre-mRNA duplex would likely obscure spliceosomal recognition of that AG), and (2) to fully base-pair with any mRNA that might originate from escaped transcripts not bound by the SSO, thus blocking and/or reducing mRNA translation. Coincidentally, the last nucleotide of the first exon is also a G. Thus, the correctly spliced AR mRNA generates the exact reverse complement of SSO753 (Figure S1B). Therefore, SSO753 can also target the AR transcripts in both the nucleus, as an SSO, and the cytoplasm, where it would function as a non-RNaseH active ASO (a.k.a. a steric blocking ASO; Figure S1B).

To determine the extent of gene silencing resulting from targeting exclusively intronic sequences, we designed an SSO (SSO815,

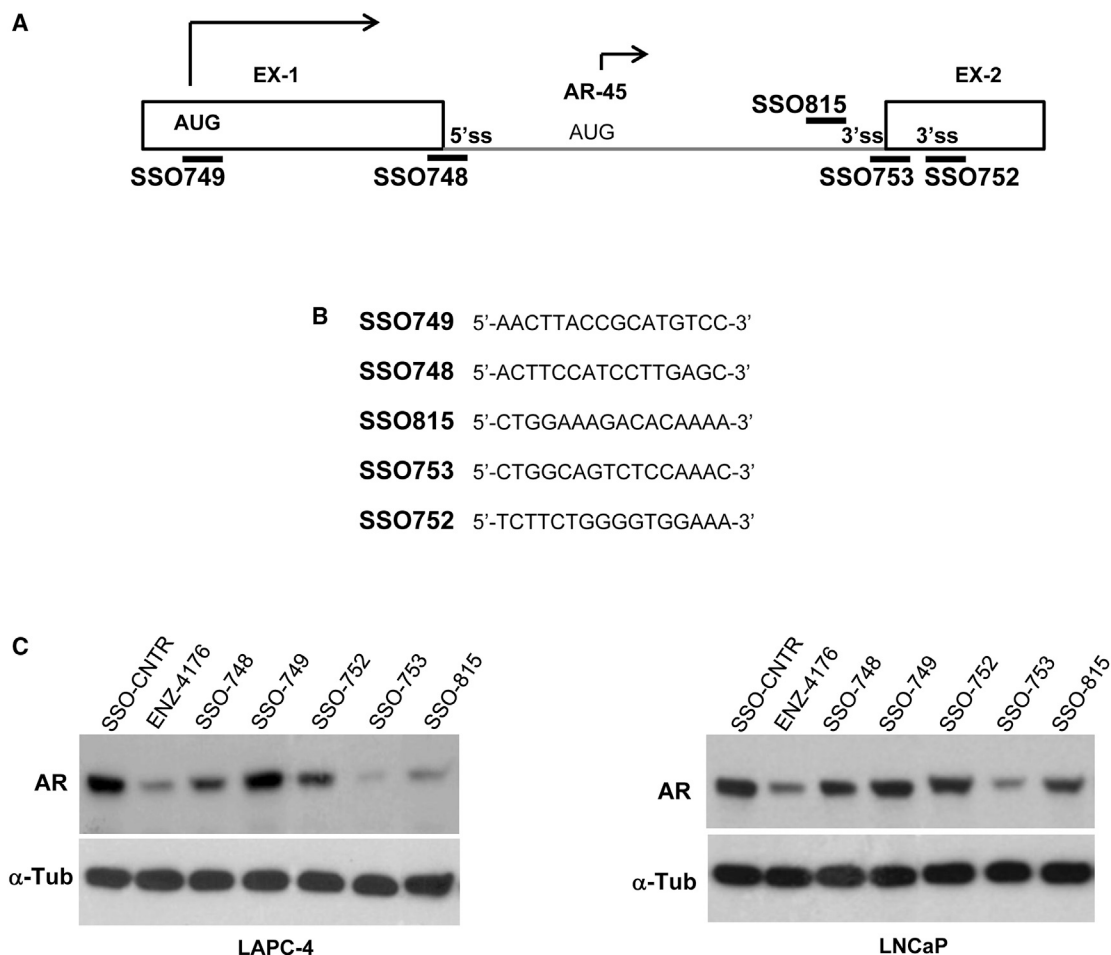


Figure 1. SSO-Based Strategies to Silence AR Gene Expression

(A) Schematic diagram of different splice-switching strategies. SSO749 blocks recognition of the endogenous translation start codon; SSO748 blocks the 5' ss of intron 1; SSO815 blocks the polypyrimidine sequence upstream of the 3' ss of intron 1; and SSO753 and SSO752 block the canonical 3' ss at the intron 1-exon 2 junction and a second alternative 3' ss within exon 2, respectively. (B) Initial SSO sequences employed in this work. (C) Representative western blot analysis showing AR protein expression in two prostate cancer cell lines (LAPC-4 and LNCaP) transfected with 20 nM of each SSO as indicated in the figure. SSO-CNTR is a non-targeting LNA PS oligonucleotide, used as a control for non-specific AR silencing. ENZ4176 is a potent AON targeting the AR mRNA, which was used as comparative control; α -tubulin is the loading control.

Figures 1A and 1B; Figure S1A) directed at the polypyrimidine tract, a regulatory sequence that plays a key role in the recognition and selection of splice sites.^{33,34} The third SSO (SSO752, Figures 1A and 1B) was designed to block a potential alternative downstream 3' ss, which, if selected, could generate a translatable ORF. The fourth SSO (SSO748, Figures 1A and 1B) was designed to base-pair and block recognition of the 5' ss. The final SSO (SSO749, Figures 1A and 1B) was designed to base-pair with and block the translation start codon of the AR mRNA. SSO749 was included to compare the extent of silencing induced by directly interfering with translation (using the SSO as a steric blocker)³⁵ to the extent of silencing resulting from translational suppression due to SSO-mediated cellular NMD. The results of these experiments indicate that the latter is a significantly more effective mechanism to silence AR gene expression (Figure 1C) than is the former.

The bi-functional SSO753 exhibited the strongest silencing activity of all SSOs (Figure 1C). In general, targeting the 3' ss (Figure 1C, SSO815, SSO753, SSO752) proved to be more effective than targeting the 5' ss (Figure 1C, SSO748). However, blocking the canonical 3' ss could not prevent engagement of the 5' ss by the spliceosome and the potential selection of an alternative intronic AG. This abnormal splicing reaction would still result in the inclusion of PTCs (we confirmed that no other ORF can form) and subsequent degradation of the AR RNA, but it would diminish/eliminate the likelihood of generating AR45 transcripts.

AR45 is the only known AR isoform that does not contain exon 1¹³ and does not exhibit oncogenic activity.¹⁹ In place of exon 1, AR45 contains exon 1b, which encodes a 7-aa-long peptide sequence unique to this isoform.¹⁹ AR45 appears to form heterodimers with the NTDs

of other AR isoforms, acting as an antagonist and blocking AR function.¹⁹ It is possible that preventing the splicing reaction from occurring at the canonical 5' splice site of the AR transcript could grant sufficient time for the alternative 5' splice site of exon 1b to splice and generate the AR45 transcript. This presents an opportunity to design a second bi-functional SSO that would degrade the AR RNA transcripts (due to the partial intron retention), while at the same time favoring production of the AR antagonist AR45. Ribosome binding to the canonical translation start site would encounter premature stop codons, hence triggering NMD. Whereas ribosome binding to the exon 1b internal start site (prior to any transcript degradation), would allow translation to occur and AR45 expression. To test whether SSO748 possessed this dual function, we performed a series of qRT-PCR reactions to analyze the AR pre-mRNA and mRNA transcripts resulting from SSO treatment of LNCaP cells (Figures S2A and S2B). The PCR primers were designed to specifically amplify the AR-FL or the AR45 transcripts. The data show that all SSO treatments resulted in a decrease of AR gene expression (Figure S2B). SSO748, the only SSO targeting the 5' splice site, was shown, in fact, to be a bi-functional oligonucleotide, as it could also generate AR45 transcripts (Figure S1B).

Optimization of SSO Function through Design Modeling and Empirical Screens

After determining the feasibility of the strategy, we then optimized SSO potency. The data were consistent with the bi-functional SSOs being the most potent. Therefore, we selected those two targeted regions (the 5' splice site [748 series of SSOs] and 3' splice site [753 series of SSOs] of intron 1) to design a screen of approximately 250 oligonucleotides. The sequence, length, and location of the LNA modifications were varied based on a proprietary modeling prediction program (developed by Roche Innovation Center, Copenhagen, Denmark). The resulting SSOs were used to treat different PCa cell lines. Subsequently, their activity was assessed via qRT-PCR and western analyses (examples of these screens are shown in Figures S3A, S3B, S4A, and S4B). The leading SSOs from the 753 series were chosen based on their ability to silence AR expression (e.g., Figures S3A and S3B), as they were not expected to generate AR45. The leading SSOs from the 748 series, however, were selected based not only on their ability to silence AR expression, but also to generate AR45 transcripts. We screened for SSOs that produced the strongest AR silencing and the best simultaneous AR45 expression. The latter was established for both AR45 absolute expression and AR45 expression as a percentage of the remaining AR. For example, SSO363 was preferable to SSO362 (Figure S4B, left graph) because even though they down-regulated AR expression to the same extent, SSO363 generated a higher expression of AR45 (Figure S4B, left graph). However, SSO372 was preferable to SSO376 (Figure S4B, right graph), despite producing a lower overall expression of AR45. This is because, when analyzed by the percentage of residual AR transcripts, cells treated with SSO372 still demonstrated a greater AR45/AR-FL ratio. Moreover, AR silencing was better achieved after SSO372 treatment (compare SSO372 to SSO376; Figure S4B, right graph).

Based on the above results, we chose the eight most active SSOs (Figures S5; Figure 2). By combining the modeling program and the

empirical screen, we were able to identify 5' splice site-targeting SSOs (748 series) that were as effective as the 753 series in silencing AR expression (Figures 2A and 2B; compare SSO407, SSO390, SSO410, and SSO395 with SSO541, SSO480, SSO547, and SSO111) and as potent as an ASO control (ENZ-4176, Figures 2A and 2B). SSOs belonging to the 748 series also increased expression of AR45 mRNA (Figure 2B, SSO407, SSO390, SSO410, and SSO395). To determine whether the reduction in AR gene expression was reflected in the regulation of AR-responsive promoters, we delivered the selected SSOs to LNCaP cells previously engineered to express an AR-responsive luciferase gene (see Materials and Methods). All SSO treatments reduced luciferase expression, with SSO541 and SSO407 being the most effective (Figure 2C). Under our experimental conditions, none of the SSOs showed any significant treatment-related toxicity in the PCa cell lines used for this work (Figures 3A and 3B and data not shown).

The potency of the eight most active SSOs was also assessed and confirmed in LAPC-4 cells (Figures 4A [748 series] and 4B [753 series]) and 22RV1 cells (Figures 4C [748 series] and 4D [753 series]). The 22RV1 PCa line expresses ARv7,³⁶ the most prominent AR mutation found in later stage PCa patients. Notably, all selected SSOs were able to diminish expression of the ARv7 isoform (Figures 4C and 4D).

Reduced AR Expression Is Reflected in the Downregulation of AR-Responsive Cellular Genes

The most potent four (Figures 2A–2C and 4A–4D; SSO390, SSO407, SSO457, and SSO541) out of the eight previously selected SSOs were further tested in serial dilution experiments to identify the best overall SSO for the 753 and 748 series (to be carried forward for *in vivo* studies). SSO407 and SSO541 were effective at lower concentrations (Figure 5A). Furthermore, serial dilutions of SSO407 appeared to exhibit an inverse relationship between the expression of AR and AR45 (Figures 5B and 5C). These results were consistent with the appearance of an approximately 45-kDa molecular weight product, which increased as the AR-FL detection decreased (Figure S6A).

Finally, we corroborated the potency of the SSOs by determining the degree to which two AR-responsive endogenous cellular genes, prostate-specific antigen (PSA) and transmembrane serine protease 2 (TMPRSS2), are affected by SSO-driven AR silencing. All SSOs reduced expression of the AR-regulated PSA and TMPRSS2 genes, with the best outcomes obtained using SSO541 and SSO407 (Figure 6). The reduced expression may reflect elimination of the AR-gene transactivation and a return to a more canonical endogenous expression. Importantly, even a modest, but simultaneous decrease in gene expression of multiple AR-responsive genes could have a significant impact on blocking PCa progression.

SSO541 and SSO407 were then evaluated in a small *in vivo* pilot study, in which four groups of six NSG mice were subcutaneously grafted with LNCaP tumors of comparable sizes. The mice were treated with either the delivery medium (1 × PBS) for the injections (vehicle), a non-targeting control oligonucleotide (SSO-control [CNTR]), or either SSO541 or SSO407 (Figure S6B). The treatment

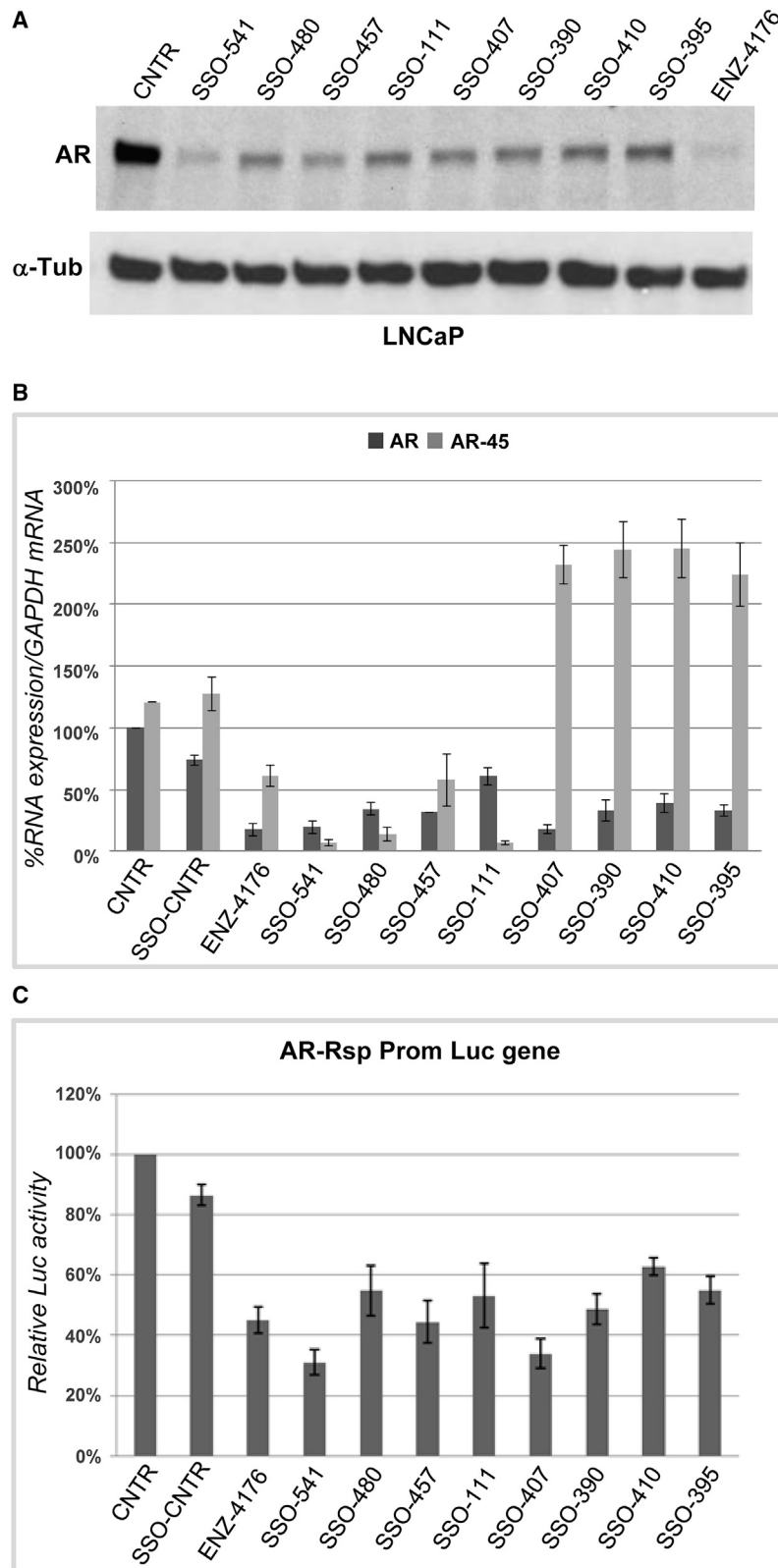


Figure 2. SSO-Mediated AR Regulation

(A) Representative western blot analyses of lysates harvested from LNCaP cells treated for 2 days with 20 nM of each specific SSO (as indicated in the figure). α -Tubulin was used as the loading control. The experiment was repeated several times with comparable results. (B) LNCaP cells were transfected with the AR-responsive luciferase gene and 20 nM of each SSO (as indicated in the graph) for 48 h; total RNA was then harvested for AR and AR45 mRNA qRT-PCR. The non-treated cells and the SSO-CNTR-treated cells were used as reference groups. Values were normalized to GAPDH mRNA expression and expressed as the mean \pm SD; n = 3. p values for changes in AR expression were as follows: ENZ-4176, p = 0.002; SSO541, p = 0.007; SSO480, p = 0.009; SSO457, p = 0.002; SSO111, p = 0.002; SSO407, p = 0.002; SSO390, p = 0.008; SSO410, p = 0.02; SSO395, p = 0.007. p values for changes in AR-45 expression were as follows: ENZ-4176, p = 0.005; SSO541, p = 0.006; SSO480, p = 0.003; SSO457, p = 0.01; SSO111, p = 0.004; SSO407, p = 0.008; SSO390, p = 0.004; SSO410, p = 0.007; SSO395, p = 0.006. (C) An LNCaP cell line expressing an AR-responsive luciferase gene was transfected with 20 nM of each SSO (as indicated in the graph). Cells were harvested 48 h after treatment and analyzed using a Dual-Luciferase assay system. Any decrease of luciferase expression represents an equivalent loss of AR nuclear transactivation activity, which in turn is caused by SSO-mediated AR silencing. Therefore, the extent of luciferase silencing reflects the degree of SSO potency. Values are expressed as the mean \pm SD; n = 3. p values for changes in luciferase units were: ENZ-4176, p = 0.007; SSO541, p = 0.01; SSO480, p = 0.007; SSO457, p = 0.0002; SSO111, p = 0.009; SSO407, p = 0.0002; SSO390, p = 0.017; SSO410, p = 0.02; SSO395, p = 0.038. The non-targeting SSO-CNTR was used as a negative control, and ENZ4176 served as the positive control. Samples SSO541, SSO480, SSO457, and SSO111 target the 3' ss of intron 1. Samples SSO407, SSO390, SSO410, and SSO395 target the 5' ss of intron 1.

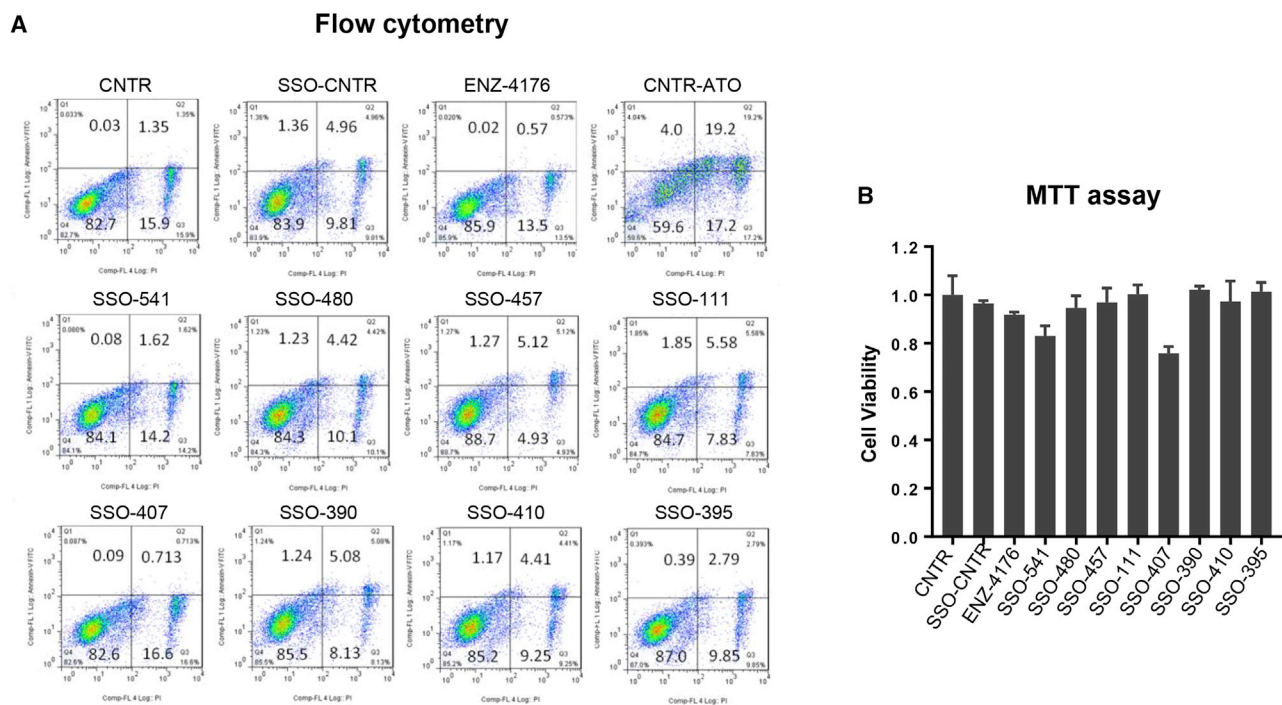


Figure 3. Apoptosis and Cytotoxicity (MTT) Assays of SSO-Transfected LNCaP Cells

(A and B) Flow cytometry (A) and MTT (B) assays were performed to determine potential SSO-driven cytotoxicity. An untreated sample (CNTR) and the non-targeting SSO-CNTR were included as negative controls. A sample (CNTR-ATO) treated with 2 μ M arsenic trioxide to induce cell apoptosis, was included as positive control. The profiles shown for the SSOs are typical of three independent experiments and are comparable to the controls, indicating no significant toxicity under the conditions of these experiments.

regimen consisted of three injections of limited SSO amounts (25 ng/g) during the first week. Mice were sacrificed after 3 weeks. The tumors were dissected from the animals and weighed. The average of the tumor weights for each group (Figure S6B) is indicative of the extent to which SSO-mediated AR silencing was effective *in vivo*.

DISCUSSION

The AR is expressed early in PCa and continues to be expressed throughout the course of the disease, driving the growth, metastatic capability, and anti-apoptotic phenotype of PCa cells. One of the mainstays of current clinical PCa therapy is, therefore, a reduction in the levels of plasma and intra-tumoral androgen.³⁷ This strategy, known as ADT, is initially accomplished by drugs that act at the hypothalamic-pituitary-gonadal axis. These agents lower plasma testosterone to castrate levels but do not lower intra-tumoral levels of testosterone.³⁷ On disease recurrence, patients are then often treated with oral hormonal agents such as abiraterone or enzalutamide.³⁸ The former is a potent inhibitor of CYP17, a key enzyme in the biosynthesis of testosterone from steroid precursors. The latter is a potent inhibitor of the binding of testosterone to the AR, and of the translocation of the AR to the cell nucleus.³⁸ However, all patients will eventually progress³⁹ through these treatments. Patients that progress to CRPC inevitably become refractory to PCa therapies.

ASO gapmers have previously been used to successfully silence AR expression.^{28,29,40} Some excellent work using a PCa mouse model has been performed by Yamamoto et al.²⁸ and De Velasco et al.,²⁹ who developed an effective AR ASO (IONIS-AR-2.5Rx). This ASO is currently being tested in a phase I PCa clinical trial in combination with enzalutamide. However, another gapmer (ENZ-4176) previously developed by Enzon Pharmaceuticals, which had displayed strong efficacy in mouse studies,⁴⁰ did not prove to be beneficial in a human PCa clinical trial.⁴⁰ Perhaps these discrepancies are in part due to the gapmers' central region, which must allow recognition of the DNA/RNA duplex by RNaseH2B, and as a result, cannot be chemically protected by anything more than PS linkages. Although new generations of gapmers have increased stability, systemic longevity in human blood and tissues may still be an issue. Furthermore, RNaseH2B, which is required for gapmer function, is downregulated in several cancers, including PCa.³⁰

In this work, we developed anti-AR SSOs that have nuclease-resistant modifications spaced throughout the molecule.^{41–43} Currently, there are three SSO treatments that are FDA approved: eteplirsen,^{31,44} nusinersen,^{24,45,46} and golodirsen.⁴⁷ Nuclease resistance was achieved with morpholino^{48,49} (eteplirsen and golodirsen) and the 2'-O-methoxyethyl (2'-MOE)⁴⁶ (nusinersen) PS modifications. We chose to use LNA PS modifications as they increase the melting temperature (T_m) of each modified nucleotide/complement heterodimer by 2°C–8°C,²⁵ stabilizing the oligonucleotide and its interaction with the target.^{50–52} In

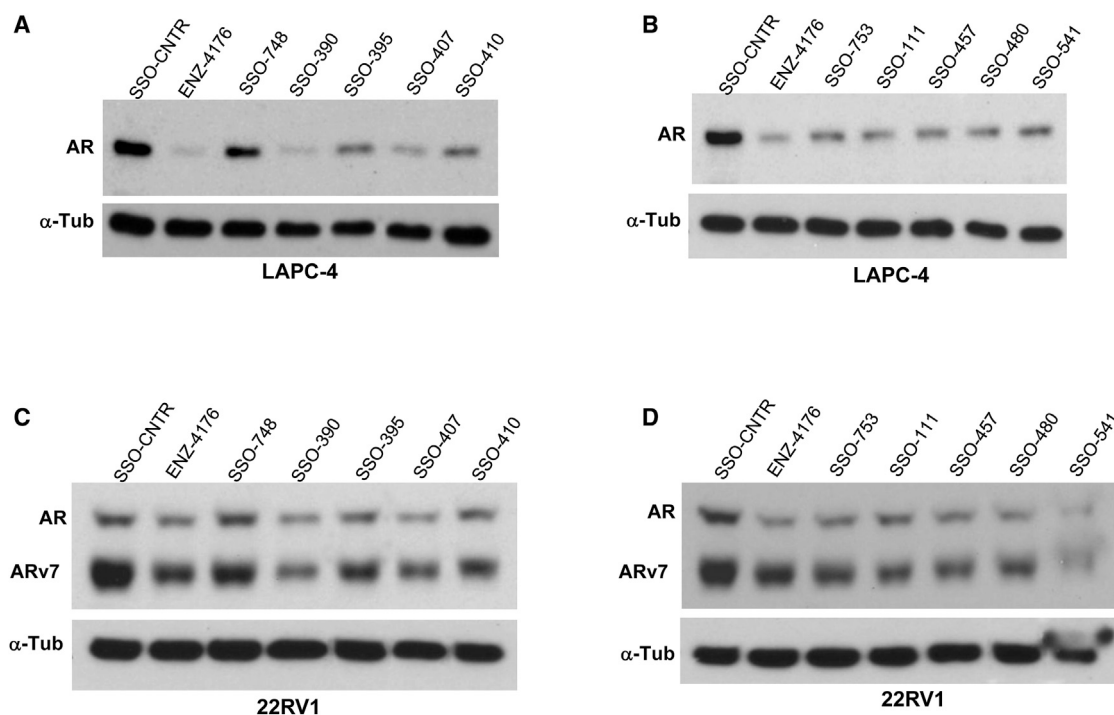


Figure 4. SSO-Mediated AR Silencing in LAPC-4 and 22RV1 Cell Lines

(A–D) Representative western blot analyses of lysates harvested from LAPC-4 cells (A and B) and 22RV1 cells (C and D), which had been treated for 2 days with 20 nM of each specific SSO (as indicated in the figure). The SSO target was either the canonical 5' ss (A and C) or the canonical 3' ss (B and D) of intron 1. The ARv7 isoform was expressed and detected in the 22RV1 cell line only (C and D). α -Tubulin was used as the loading control.

addition to significantly increased metabolic stability, LNA modifications impart improved pharmacokinetic properties to the molecule.^{53,54} Lastly, because the binding of LNA-modified oligonucleotides to their targets is not particularly affected by point mutations, an LNA-PSO strategy is not expected to produce the same drug resistance that currently employed chemotherapy treatments do.

Our strategy seeks to destabilize the AR RNA transcripts, while enhancing production of the AR45 mRNA, using a single therapeutic molecule. Our tailor-made SSOs successfully generated AR45 mRNA (Figures 2 and 5; Figures S2 and S4). Although AR45 production is not required to achieve strong AR silencing (e.g., SSO541, Figures 2, 4, 5, and 6), it could further improve suppression of AR transactivation, extend the length of silencing time, and/or lower the SSO concentration required for therapy.

Mass spectrometry (MS) analysis of immune precipitates from CNTR-, SSO-CNTR-, and SSO407-treated cell lysates using an anti-AR antibody confirmed an overall AR reduction in the SSO407-treated cells (data not shown), while detecting upregulated proteins also unique to the SSO407 samples (Figure S7). Of particular interest is the overexpression of cornulin (CRNN), also known as C1orf10, which was only detected in the AR-targeting, SSO-treated LNCaP cells. CRNN is a stress response protein⁵⁵ whose induction suppresses cell proliferation and causes a G₁ phase cell cycle arrest,^{56,57} in part through the down-

regulation of cyclin D1 expression.⁵⁶ The latter is an oncogene that has been implicated in a variety of cancers, including Pca.⁵⁸ Therefore, CRNN plays an important role in carcinogenesis as a tumor suppressor. It is not clear why SSO-mediated AR downregulation leads to CRNN overexpression, but this is certainly a valuable outcome of this SSO strategy. Another interesting observation is that silencing of AR expression starts to reinstate RNaseH2B expression (Figure S7B). RNaseH2B is generally downregulated in Pca,³⁰ but it appears upregulated in SSO407-treated cells when compared to the non-treated and the non-targeting SSO-treated cells (Figure S7B).

The AR and its splicing variants (with the exception of AR45) all contain the NTD encoded by exon 1 and translocate to the nucleus. Survival genes, including PSA,⁵⁹ FGF8,⁶⁰ Cdk1 and Cdk2,⁶¹ PMEPA1,⁶² and TMPRSS2⁶³ are then transactivated, ultimately leading to CRPC. The SSOs developed in this work target the first intron, and thus can alter splicing of all AR alternative spliced isoforms. We also consistently show that the stability of ARv7 transcripts can be reduced by SSO treatment (22RV1 cells, Figure 4B). This particular splice variant continuously activates the expression of cell survival genes and leads to poor patient outcomes.³⁶ The reduced expression of this variant is a much sought-after goal of Pca therapy. Furthermore, AR45, which forms heterodimers with the NTD, could also act as an antagonist against all CRPC-related AR isoforms.

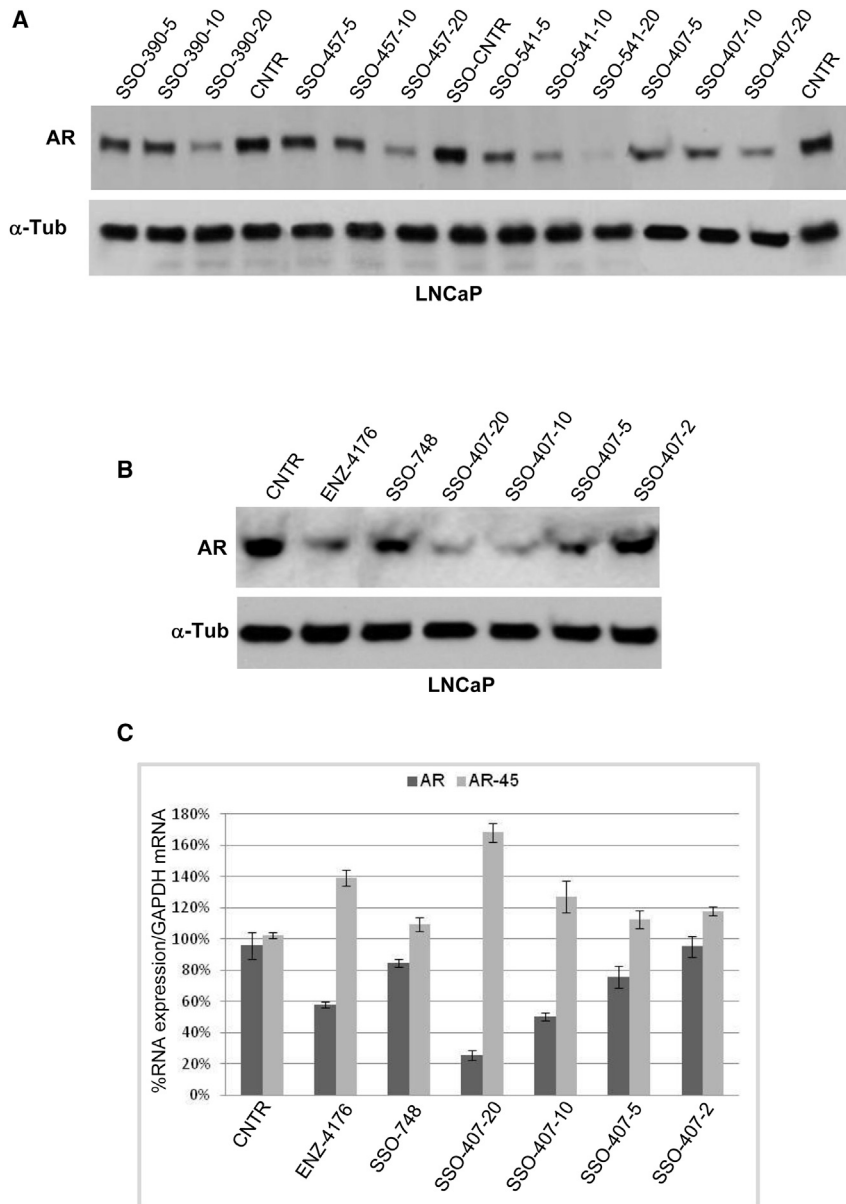


Figure 5. SSO Concentration Dependence on AR Gene Expression

(A and B) Representative western blot analysis of lysates harvested from LNCaP cells treated for 2 days with 5, 10, and 20 nM (A) and 2, 5, 10, and 20 nM (B) of each SSO, as illustrated in the figure. Western blot analysis shows a concentration-dependent SSO-mediated reduction of AR protein expression, with SSO541 (targeting the 3' ss) and SSO407 (targeting the 5' ss) being the most potent at the lower concentrations (compare SSO541 [10 nM] with SSO390 [10 nM] and SSO407 [5 nM] with SSO457 [5 nM]). α -Tubulin serves as the loading control. (C) LNCaP cells were transfected with decreasing concentrations (20, 10, 5, and 2 nM) of SSO407 for 48 h. Total RNA was then harvested for AR and AR45 mRNA qRT-PCR. The data show an SSO-mediated concentration-dependent reduction of AR mRNA expression, which is mirrored by an increase in AR45 expression. The experiments were done in triplicates and all values were normalized to the internal control (GAPDH). Non-treated cells (CNTR) were used as reference group for the treatments, and ENZ4176 was used as positive control. Both controls were transfected at the highest concentration (20 nM).

MATERIALS AND METHODS

Cells, Culture Conditions, and Reagents

The PCa cell lines LNCaP, 22Rv1, and LAPC-4 were cultured in RPMI 1640 (Media Tech/Celgro) supplemented with 10% fetal bovine serum (FBS) and 2 mM L-glutamine. LNCaP and LAPC-4 cells were cultured on dishes or plates coated with PBS containing 0.01% poly-lysine (Sigma-Aldrich, St. Louis, MO, USA) to facilitate cell growth. All cell line cultures were maintained at 37°C in a humidified 5% CO₂ incubator.

One day prior to transfection, cells were seeded at 60% confluence in RPMI 1640 containing 10% FBS. The SSOs were delivered at a final concentration of 5–20 nM using Lipofectamine 3000 (Thermo Fisher Scientific, Waltham, MA, USA)

following the manufacturer's recommendations. Cells were harvested 48 h after SSO transfection for western blotting and qRT-PCR.

A list of all SSO sequences screened in this work is available upon request.

The primary antibodies used in this work were as follows: AR antibody (441) from Santa Cruz Biotechnology, GAPDH antibody (D16H11) from Cell Signaling Technology (Boston, MA, USA), and anti- α -tubulin antibody from Sigma-Aldrich (St. Louis, MO, USA). Secondary antibodies against rabbit (NA934) and mouse (NA931) primary antibodies were purchased from GE Healthcare.

Preliminary data suggest that SSO407, which can lead to the production of AR45, performs slightly better than SSO541 *in vivo* (Figure S6B). In future experiments, a larger cohort of mice will be treated with SSO407 and SSO541 to confirm these observations. They will be evaluated alone or combined with As III and NH₄⁺, two FDA-approved drugs that we previously demonstrated to increase ASO and SSO potency.^{64,65} If proven effective *in vivo*, our bi-functional AR SSO design could become the basis for a new type of treatment of androgen-independent PCa. Importantly, this strategy can potentially be customized to other types of therapies that require the silencing of one gene and the simultaneous expression of another, as long as these genes share a common pre-mRNA transcript.

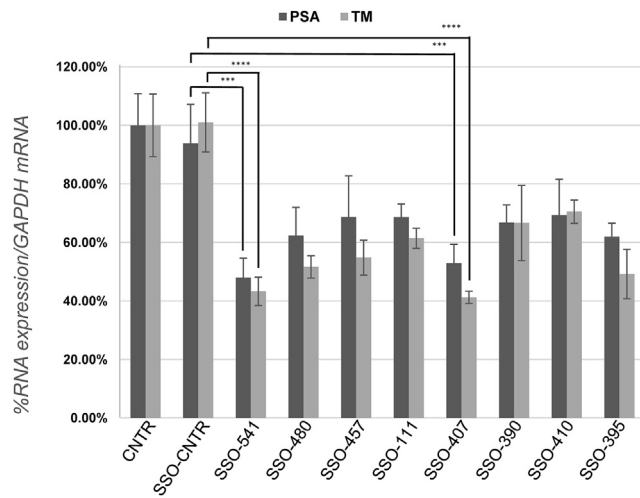


Figure 6. Levels of Expression of mRNA for AR-Regulated Genes after SSO Treatment

Levels of prostate-specific antigen (PSA) mRNA and TMPRSS2 (TM) mRNA were measured by qRT-PCR. LNCaP cells were transfected with 20 nM SSO and harvested for RNA isolation 48 h later. qRT-PCR was performed using the SYBR Green assay. All samples were first normalized to GAPDH as an internal control and then to the untreated (UNTR) samples. The non-targeting ON, SSO-CNTR, was used as a negative control. Samples SSO541, SSO480, SSO457, and SSO111 targeted the canonical 3' ss of intron 1. Samples SSO407, SSO390, SSO410, and SSO395 targeted the canonical 5' ss of intron 1. The experiment was performed three times in triplicate. Statistical analysis was performed using an unpaired t test (PSA-SSO541, $p = 0.0003$; PSA-SSO407, $p = 0.0005$; TM-SSO541, $p < 0.0001$; TM-SSO407, $p < 0.0001$).

Western Analysis

Generally, cells were harvested 48 h after treatment by trypsin digestion following a washing step with PBS. Cell pellets were lysed using cold radioimmunoprecipitation assay (RIPA) buffer containing protease inhibitors followed by 2 s of sonication and a 5-min incubation on ice. After removal of cell debris by centrifugation at 4°C, protein concentrations were determined using the Pierce bicinchoninic acid (BCA) protein assay kit (Thermo Fisher Scientific, Waltham, MA, USA). Aliquots of cell extracts containing 25–50 µg of protein were resolved by 4%–20% precast polyacrylamide gels purchased from Bio-Rad (Hercules, CA, USA) and imaged using chemiluminescence. The dilution of the various antibodies followed the manufacturers' instructions. The monoclonal mouse anti-human α -tubulin antibody (Sigma-Aldrich) was added at 4,000 \times dilution in Tris-buffered saline with Tween 20 (TBST) containing 5% fat-free dry milk. Protein signals on the blot were quantified with the ImageJ program and protein expression was normalized to the SSO control.

qRT-PCR

Total RNA from LN-CAP cells was extracted using RNA-STAT60 (Tel-Test, Friendswood, TX, USA, or AMS Biotechnology, Abingdon, UK) according to the manufacturers' recommendations. The RNA was treated with Turbo DNase I (Ambion, Foster City, CA, USA) or digested with Ambion DNase I (Thermo Fisher Scientific, Wal-

tham, MA, USA) to eliminate residual DNA according to the manufacturer's instructions. First-strand cDNA was obtained by reverse transcribing 2 µg of total RNA with iScript reverse transcriptase (Bio-Rad, Hercules, CA, USA). Fifty nanograms of the resulting cDNA was analyzed via qRT-PCR using Power SYBR Green PCR master mix (Thermo Fisher Scientific, Waltham, MA, USA) or SsoAdvanced SYBR Green supermix (Bio-Rad, Hercules, CA, USA) with the corresponding specific primer sets. PCR was performed for 40 cycles at an annealing temperature of 60°C for 45 s, followed by a melting curve analysis. mRNA levels were normalized to the level of endogenous glyceraldehyde 3-phosphate dehydrogenase (GAPDH) mRNA, which served as an internal control. Values were determined from the calculated threshold cycle using the CFX Maestro software from Bio-Rad (Hercules, CA, USA). Each sample was analyzed in triplicate.

The PCR primers were as follows: AR 45-56 (5'-CCTGGCTTCCGCAACTTACAC-3', 5'-GGACTTGTGCATGCGGTACTCA-3' and 5'-CGCACAGGTACTTCTGTTTCC-3', 5'-GGACTTGTGCATGCGGTACTCA-3'), AR-V7 (5'-CCATCTTGTGCTCTTCGGAAATGTTA-3', 5'-TTTGAATGAGGCAAGTCAGCCTTTCTC-3'),¹² AR45 P1 (5'-CGAGCAGAGAGG GATTCTCTGGAGG-3', 5'-CCTGGCAGTCTCCAAACTGTGAAGCC-3'), AR45 P2 (5'-ATGATACTCTGGCTTCACAG-3', 5'-GCGGCTCTTTTGAAGAAGAC-3'), PSA (5'-TCTGCGGCGGTGTTCTG-3', 5'-GCCGACCCAGCAAGATCA-3'), TSPRSS2 (5'-GGACAGTGTGCACCTCAAAGAC-3', 5'-TCCCACGAGGAAGTCCC-3'), GAPDH (5'-AGGTGAAGTTCGGAGTCAAC-3', 5'-ATCTCGCTCCTGGAAGATGG-3').

Dual-Luciferase Assay

LNCaP cells were transduced using the Cignal Lenti AR reporter (Luc) kit (catalog no. CLS-2020L, product no. 336851; QIAGEN, CA, USA) following the manufacturer's recommendations. The lentiviral reporter expresses an AR-responsive luciferase gene, which reflects AR transactivation activity. Transduced cells were later transfected with 20 nM selected SSOs and harvested 48 h after treatment. Dual-Luciferase activities were determined by the Dual-Luciferase assay systems as per the manufacturer's protocol (Promega, Madison, WI, USA).

Flow Cytometry Analysis and Cell Viability

LNCaP cells were treated for 2 days with the various SSOs as indicated in Figure 3. Cell apoptosis assays were performed with Annexin V-FITC Apoptosis Staining / Detection Kit (Abcam). Cells treated for two days with 2 µM Arsenic trioxide served as a positive control for apoptosis. Flow cytometry data were collected using a CyAn flow cytometer (Beckman Coulter, Brea, CA, USA) and analyzed with FlowJo software (Tree Star, Ashland, OR, USA) to determine fluorescence intensity versus cell number. Cell growth and viability assays were performed with CellTiter 96 AQ_{ueous} One solution (Promega, Madison, WI, USA). For CellTiter 96 AQ_{ueous} assays, cells were seeded into 96-well plates and treated as indicated for 2 days. 20 µL of CellTiter 96 AQ_{ueous} reagent was added to each well and

incubated at 37°C for 1–2 h prior to recording the absorbance at 490 nm with a microplate reader.

Immunoprecipitation

LNCaP cell lines were seeded at about 50% confluency in 10-cm dishes. Approximately 24 h later, 40 nM SSOs (final concentration) were transfected using Lipofectamine 3000 (Thermo Fisher Scientific, Waltham, MA, USA) as recommended by the manufacturer. After 48 h, the dishes were placed on ice, the media were removed, and the cells were washed twice with 10 mL of cold PBS. Cells were lysed by adding 600 μ L of cold RIPA buffer (Bio-Rad, Hercules, CA, USA) including protease inhibitor (protease inhibitor tablets were purchased from Thermo Fisher Scientific, Waltham, MA, USA) directly to the cells. After about 10 min of incubation on ice, cells were scraped and collected into tubes. Samples were frozen overnight to facilitate complete lysis. The next day, cell debris was removed by centrifugation at 4°C and 13,000 rpm for 15 min (Eppendorf refrigerated centrifuge 5418 R). The supernatant/lysate was then transferred to cold, fresh tubes. Protein concentrations were determined using the Pierce BCA protein assay kit (Thermo Fisher Scientific, Waltham, MA, USA). Immunoprecipitation was performed using the Dynabeads co-immunoprecipitation (coIP) kit by Thermo Fisher Scientific (Waltham, MA, USA) as recommended by the manufacturer, with the following adjustments.

1.5 mg of beads per sample was weighed and transferred into a microcentrifuge tube. Beads were washed with 1 mL pf C1 buffer, the tube was placed into a magnet, and the supernatant was removed once clear. To covalently couple the antibody to the beads, 1 mL of C2 buffer, 969 μ L of C1 buffer, and 31 μ L of anti-AR antibody (C terminus, EP670Y, Abcam, Cambridge, UK) were added to the beads (corresponds to 3 μ g of antibody per 1 mg of beads). The beads-antibody mix was incubated overnight at 37°C with rotation. The next day, the beads were placed into the magnet and supernatant was removed once clear. At room temperature, the beads were washed first with 800 μ L of HB buffer and then 800 μ L of LB buffer, both containing 0.05% Tween 20. After removal of the supernatant, two short washes and one 15-min wash with 800 μ L of SB buffer followed. The 15-min wash was performed on a rotator at room temperature. Finally, the beads were placed in the magnet, the supernatant was removed, and the beads were resuspended in 100 μ L of SB buffer per milligram of beads.

No detergent was added to the extraction buffer. Cell lysate containing 1 mg of protein was used per sample and the final elution was performed with 30 μ L of EB buffer (Dynabeads kit, Thermo Fisher Scientific, Waltham, MA, USA).

Proteomics Sample Preparation

Eluates of control, scrambled oligonucleotide, and AR immunoprecipitations were subjected to the single-pot, solid-phase-enhanced sample preparation (SP3) method for proteomics analysis as previously described.⁶⁶ Briefly, eluates were first denatured with 8 M urea, then reduced with 5 mM dithiothreitol (DTT), and finally alkyl-

lated using 20 mM iodoacetamide (IAA), all in 50 mM HEPES buffer (pH 8). Unreacted IAA was quenched using 5 mM DTT. Samples were then subjected to SP3 clean-up using an equal mixture of rinsed Sera-Mag beads (GE Healthcare, catalog nos. 45152105050250 and 65152105050250) at a final concentration of 1 μ g/ μ L. Following addition of ethanol (final concentration 50%), samples were briefly incubated with shaking and then placed on a magnetic rack to remove the supernatant. The beads were rinsed twice with 80% ethanol, and the supernatant was discarded. Samples were then digested overnight with trypsin (Trypsin Gold, MS grade, Promega) on a ThermoMixer (Eppendorf), at 37°C and 1,000 rpm. On the following day, the samples were centrifuged at 20,000 \times g for 1 min. The peptide-containing supernatant was transferred into fresh tubes and vacuum concentrated (Eppendorf Vacufuge plus) to dryness.

Liquid Chromatography-Tandem MS (LC-MS/MS)

Dried peptides were reconstituted in 2% acetonitrile, 0.1% formic acid containing 25 fmol of Pierce peptide retention time calibration (PRTC) mixture. MS data were acquired on an FAIMS Pro (high-field asymmetric waveform ion mobility spectrometry) and advanced peak detection (APD)-enabled Orbitrap Eclipse mass spectrometer (Thermo Fisher Scientific) coupled to an Ultimate 3000 ultra high-performance liquid chromatograph (UHPLC) system (Thermo Fisher Scientific) running binary solvent system A (H₂O, 0.1% formic acid) and B (acetonitrile, 0.1% formic acid). Peptides were injected directly (5 μ L, 18.3 min loading time) on a C18 analytical column (EasySpray ES801A, 50- μ m inner diameter [ID] \times 15 cm, 2- μ m particle size, 100-Å pore size) kept at 45°C, and separated at a flow rate of 300 nL/min using a gradient of 75 min: 2% to 5% B in 5 min, 5% to 19% B in 37 min, 19% to 30% B in 6 min, 30% to 90% B in 0.5 min, plateau at 90% B for 1 min, return to initial conditions in 11.5 min, and re-equilibration for 15 min. All MS data were acquired in data-dependent top speed mode with a 1-s duty cycle per FAIMS compensation voltage (CV). The FAIMS device was operated in standard mode with three CVs at -40, -60, and -80 V and the following parameters per FAIMS CV: spray voltage of 2,000 V, ion transfer tube temperature of 305°C, survey scan in the Orbitrap Eclipse mass spectrometer at a resolution of 120,000, scan range of 375–1,575 *m/z*, standard automatic gain control (AGC) target, and auto maximum ion injection time. Every parent scan was followed by a daughter scan using high-energy collisional dissociation (HCD) of top abundant peaks and detection in the ion trap with the following settings: quadrupole isolation mode enabled, isolation window at 1.6 *m/z*, standard AGC target with auto maximum ion injection time, and HCD collision energy of 32%. Dynamic exclusion was set to 60 s.

Peptide and Protein Identification

Mass spectra were queried against the human protein sequence database (SwissProt/UniProtKB 2017, 42,150 entries) using the Mascot⁶⁷ search engine (version 2.6) in Proteome Discoverer 2.2.0.388 with the following parameters: 10 ppm precursor mass tolerance, 0.6 Da fragment mass tolerance, tryptic peptide cleavage with up to two missed internal cleavage sites, methionine oxidation as a dynamic modification, and cysteine carbamidomethylation as a static modification.

Peptide spectrum matches were filtered using Percolator (version 3.0)⁶⁸ to a 1% target false discovery rate (FDR). Intensity-based protein abundance was calculated using the precursor ion quantifier node, and abundances were normalized using the iterative rank order normalization (IRON) approach.⁶⁹ Potential contaminants listed in the CRAPome database⁷⁰ with an average spectral count greater than 10 were not retained for differential analysis.

LNCaP Xenograft Mice

LNCaP cells were grown in the exponential phase and resuspended in serum-free, antibiotic-free media. Ten-week-old NSG male mice were each injected with 5 million LNCaP cells mixed (1:1) with Matrigel (Corning Life Sciences, Corning, NY, USA), in a total volume of 100 μ L (Institutional Animal Care and Use Committee [IACUC] #18068). Inoculations were performed into the mouse flank and calipers were used to monitor tumor growth. Mice were divided into four groups: a vehicle control, SSO-CNTR, SSO407, and SSO541 and sorted at six per cage. Treatments started when tumors reached 100 mm³. Three injections of SSOs, at a concentration of 25 ng/g in a saline solution, were given to the mice only during the first week. Tumor measurements were taken every other day for 3 additional weeks. Mice were euthanized, tumors were removed, and their weights were used to determine SSO antitumor activity.

SUPPLEMENTAL INFORMATION

Supplemental Information can be found online at <https://doi.org/10.1016/j.omtn.2020.10.032>.

ACKNOWLEDGMENTS

We are grateful to Dr. Jun Wu and Yuming Guo for their assistance with the mouse studies. Research performed in the Mass Spectrometry & Proteomic and Animal Facility Cores was supported by the National Cancer Institute of the National Institutes of Health under award number P30CA033572. This work was supported by funding from Hoffmann Roche Innovation Center awarded to D.C. and C.A.S. The content is solely the responsibility of the authors and does not necessarily represent the official views of the National Institutes of Health.

AUTHOR CONTRIBUTIONS

Conceptualization, D.C. and C.A.S.; Methodology, D.C., B.R.H., T.K., P.P., R.S., and C.A.S.; Validation, X.Z., J.R., J.A., and L.J.; Formal Analysis, D.C., J.A., J.R., P.P., and R.S.; Investigation, X.Z., J.R., J.A., R.S., L.J., S.I., M.S.N., and J.V.; Resources, P.P., J.V., B.R.H., T.K., M.A.J., and J.J.R.; Writing – Original Draft, D.C. and C.A.S.; Writing–Review & Editing, M.S.N. and S.I.; Visualization, X.Z., D.C., J.R., J.A., R.S., and S.I.; Supervision, D.C., P.P., B.R.H., T.K., M.A.J., J.J.R., and C.A.S.; Funding Acquisition: D.C. and C.A.S.

DECLARATION OF INTERESTS

The authors declare no competing interests.

REFERENCES

1. Rawla, P. (2019). Epidemiology of prostate cancer. *World J. Oncol.* 10, 63–89.

- Siegel, R.L., Miller, K.D., and Jemal, A. (2020). Cancer statistics, 2020. *CA Cancer J. Clin.* 70, 7–30.
- Sadi, M.V., Walsh, P.C., and Barrack, E.R. (1991). Immunohistochemical study of androgen receptors in metastatic prostate cancer. Comparison of receptor content and response to hormonal therapy. *Cancer* 67, 3057–3064.
- Ruizeveld de Winter, J.A., Janssen, P.J., Sladdens, H.M., Verleun-Mooijman, M.C., Trapman, J., Brinkmann, A.O., Santerse, A.B., Schröder, F.H., and van der Kwast, T.H. (1994). Androgen receptor status in localized and locally progressive hormone refractory human prostate cancer. *Am. J. Pathol.* 144, 735–746.
- Attard, G., Swennenhuis, J.F., Olmos, D., Reid, A.H., Vickers, E., A'Hern, R., Levink, R., Coumans, F., Moreira, J., Riisnaes, R., et al. (2009). Characterization of ERG, AR and PTEN gene status in circulating tumor cells from patients with castration-resistant prostate cancer. *Cancer Res.* 69, 2912–2918.
- Dai, C., Heemers, H., and Sharifi, N. (2017). Androgen signaling in prostate cancer. *Cold Spring Harb. Perspect. Med.* 7, a030452.
- Hu, R., Dunn, T.A., Wei, S., Isharwal, S., Veltri, R.W., Humphreys, E., Han, M., Partin, A.W., Vessella, R.L., Isaacs, W.B., et al. (2009). Ligand-independent androgen receptor variants derived from splicing of cryptic exons signify hormone-refractory prostate cancer. *Cancer Res.* 69, 16–22.
- Pelekanou, V., Notas, G., Stathopoulos, E.N., Castanas, E., and Kampa, M. (2013). Androgen receptors in early and castration resistant prostate cancer: friend or foe? *Hormones (Athens)* 12, 224–235.
- Sun, S., Sprenger, C.C.T., Vessella, R.L., Haugk, K., Soriano, K., Mostaghel, E.A., Page, S.T., Coleman, I.M., Nguyen, H.M., Sun, H., et al. (2010). Castration resistance in human prostate cancer is conferred by a frequently occurring androgen receptor splice variant. *J. Clin. Invest.* 120, 2715–2730.
- Dehm, S.M., Schmidt, L.J., Heemers, H.V., Vessella, R.L., and Tindall, D.J. (2008). Splicing of a novel androgen receptor exon generates a constitutively active androgen receptor that mediates prostate cancer therapy resistance. *Cancer Res.* 68, 5469–5477.
- Litvinov, I.V., De Marzo, A.M., and Isaacs, J.T. (2003). Is the Achilles' heel for prostate cancer therapy a gain of function in androgen receptor signaling? *J. Clin. Endocrinol. Metab.* 88, 2972–2982.
- Antonarakis, E.S., Lu, C., Wang, H., Lubner, B., Nakazawa, M., Roeser, J.C., Chen, Y., Mohammad, T.A., Chen, Y., Fedor, H.L., et al. (2014). AR-V7 and resistance to enzalutamide and abiraterone in prostate cancer. *N. Engl. J. Med.* 371, 1028–1038.
- Lu, C., and Luo, J. (2013). Decoding the androgen receptor splice variants. *Transl. Androl. Urol.* 2, 178–186.
- Clegg, N.J., Wongvipat, J., Joseph, J.D., Tran, C., Ouk, S., Dilhas, A., Chen, Y., Grillot, K., Bischoff, E.D., Cai, L., et al. (2012). ARN-509: a novel antiandrogen for prostate cancer treatment. *Cancer Res.* 72, 1494–1503.
- Borgmann, H., Lallous, N., Ozistanbullu, D., Beraldi, E., Paul, N., Dalal, K., Fazli, L., Haferkamp, A., Lejeune, P., Cherkasov, A., and Gleave, M.E. (2018). Moving towards precision urologic oncology: targeting enzalutamide-resistant prostate cancer and mutated forms of the androgen receptor using the novel inhibitor darolutamide (ODM-201). *Eur. Urol.* 73, 4–8.
- Heidegger, I., Brandt, M.P., and Heck, M.M. (2020). Treatment of non-metastatic castration resistant prostate cancer in 2020: what is the best? *Urol. Oncol.* 38, 129–136.
- Al-Salama, Z.T. (2018). Apalutamide: first global approval. *Drugs* 78, 699–705.
- Bastos, D.A., and Antonarakis, E.S. (2019). Darolutamide for castration-resistant prostate cancer. *OncoTargets Ther.* 12, 8769–8777.
- Ahrens-Fath, I., Politz, O., Geserick, C., and Haendler, B. (2005). Androgen receptor function is modulated by the tissue-specific AR45 variant. *FEBS J.* 272, 74–84.
- Reid, J., Kelly, S.M., Watt, K., Price, N.C., and McEwan, I.J. (2002). Conformational analysis of the androgen receptor amino-terminal domain involved in transactivation. Influence of structure-stabilizing solutes and protein-protein interactions. *J. Biol. Chem.* 277, 20079–20086.
- Jenster, G., van der Korput, H.A., Trapman, J., and Brinkmann, A.O. (1995). Identification of two transcription activation units in the N-terminal domain of the human androgen receptor. *J. Biol. Chem.* 270, 7341–7346.
- Jenster, G., van der Korput, H.A., van Vroonhoven, C., van der Kwast, T.H., Trapman, J., and Brinkmann, A.O. (1991). Domains of the human androgen receptor

- involved in steroid binding, transcriptional activation, and subcellular localization. *Mol. Endocrinol.* 5, 1396–1404.
23. Simental, J.A., Sar, M., Lane, M.V., French, F.S., and Wilson, E.M. (1991). Transcriptional activation and nuclear targeting signals of the human androgen receptor. *J. Biol. Chem.* 266, 510–518.
 24. Rüger, J., Ioannou, S., Castanotto, D., and Stein, C.A. (2020). Oligonucleotides to the (gene) rescue: FDA approvals 2017–2019. *Trends Pharmacol. Sci.* 41, 27–41.
 25. Jepsen, J.S., Sørensen, M.D., and Wengel, J. (2004). Locked nucleic acid: a potent nucleic acid analog in therapeutics and biotechnology. *Oligonucleotides* 14, 130–146.
 26. Kurosaki, T., and Maquat, L.E. (2016). Nonsense-mediated mRNA decay in humans at a glance. *J. Cell Sci.* 129, 461–467.
 27. Paschalis, A., Sharp, A., Welti, J.C., Neeb, A., Raj, G.V., Luo, J., Plymate, S.R., and de Bono, J.S. (2018). Alternative splicing in prostate cancer. *Nat. Rev. Clin. Oncol.* 15, 663–675.
 28. Yamamoto, Y., Lorient, Y., Beraldi, E., Zhang, F., Wyatt, A.W., Al Nakouzi, N., Mo, F., Zhou, T., Kim, Y., Monia, B.P., et al. (2015). Generation 2.5 antisense oligonucleotides targeting the androgen receptor and its splice variants suppress enzalutamide-resistant prostate cancer cell growth. *Clin. Cancer Res.* 21, 1675–1687.
 29. De Velasco, M.A., Kura, Y., Sakai, K., Hatanaka, Y., Davies, B.R., Campbell, H., Klein, S., Kim, Y., MacLeod, A.R., Sugimoto, K., et al. (2019). Targeting castration-resistant prostate cancer with androgen receptor antisense oligonucleotide therapy. *JCI Insight* 4, e122688.
 30. Wang, C., Wang, G., Feng, X., Shepherd, P., Zhang, J., Tang, M., Chen, Z., Srivastava, M., McLaughlin, M.E., Navone, N.M., et al. (2019). Genome-wide CRISPR screens reveal synthetic lethality of RNASEH2 deficiency and ATR inhibition. *Oncogene* 38, 2451–2463.
 31. Stein, C.A., and Castanotto, D. (2017). FDA-approved oligonucleotide therapies in 2017. *Mol. Ther.* 25, 1069–1075.
 32. Kurosaki, T., Popp, M.W., and Maquat, L.E. (2019). Quality and quantity control of gene expression by nonsense-mediated mRNA decay. *Nat. Rev. Mol. Cell Biol.* 20, 406–420.
 33. Reed, R. (1989). The organization of 3' splice-site sequences in mammalian introns. *Genes Dev.* 3 (12B), 2113–2123.
 34. Coolidge, C.J., Seely, R.J., and Patton, J.G. (1997). Functional analysis of the polypyrimidine tract in pre-mRNA splicing. *Nucleic Acids Res.* 25, 888–896.
 35. Lecosnier, S., Cordier, C., Simon, P., François, J.C., and Saison-Behmoaras, T.E. (2011). A steric blocker of translation elongation inhibits IGF-1R expression and cell transformation. *FASEB J.* 25, 2201–2210.
 36. Qu, Y., Dai, B., Ye, D., Kong, Y., Chang, K., Jia, Z., Yang, X., Zhang, H., Zhu, Y., and Shi, G. (2015). Constitutively active AR-V7 plays an essential role in the development and progression of castration-resistant prostate cancer. *Sci. Rep.* 5, 7654.
 37. Villanueva, M.T. (2014). Prostate cancer: is androgen-deprivation therapy chosen wisely? *Nat. Rev. Clin. Oncol.* 11, 501.
 38. Zhang, T., Zhu, J., George, D.J., and Armstrong, A.J. (2015). Enzalutamide versus abiraterone acetate for the treatment of men with metastatic castration-resistant prostate cancer. *Expert Opin. Pharmacother.* 16, 473–485.
 39. Watson, P.A., Arora, V.K., and Sawyers, C.L. (2015). Emerging mechanisms of resistance to androgen receptor inhibitors in prostate cancer. *Nat. Rev. Cancer* 15, 701–711.
 40. Bianchini, D., Omlin, A., Pezaro, C., Lorente, D., Ferraldeschi, R., Mukherji, D., Crespo, M., Figueiredo, I., Miranda, S., Riisnaes, R., et al. (2013). First-in-human phase I study of EZN-4176, a locked nucleic acid antisense oligonucleotide to exon 4 of the androgen receptor mRNA in patients with castration-resistant prostate cancer. *Br. J. Cancer* 109, 2579–2586.
 41. Dominski, Z., and Kole, R. (1993). Restoration of correct splicing in thalassemic pre-mRNA by antisense oligonucleotides. *Proc. Natl. Acad. Sci. USA* 90, 8673–8677.
 42. Kole, R., Krainer, A.R., and Altman, S. (2012). RNA therapeutics: beyond RNA interference and antisense oligonucleotides. *Nat. Rev. Drug Discov.* 11, 125–140.
 43. Shimo, T., Tachibana, K., Saito, K., Yoshida, T., Tomita, E., Waki, R., Yamamoto, T., Doi, T., Inoue, T., Kawakami, J., and Obika, S. (2014). Design and evaluation of locked nucleic acid-based splice-switching oligonucleotides in vitro. *Nucleic Acids Res.* 42, 8174–8187.
 44. Aartsma-Rus, A., Ferlini, A., Goemans, N., Pasmooij, A.M., Wells, D.J., Bushby, K., Vroom, E., and Balabanov, P. (2014). Translational and regulatory challenges for exon skipping therapies. *Hum. Gene Ther.* 25, 885–892.
 45. Hua, Y., Sahashi, K., Hung, G., Rigo, F., Passini, M.A., Bennett, C.F., and Krainer, A.R. (2010). Antisense correction of SMN2 splicing in the CNS rescues necrosis in a type III SMA mouse model. *Genes Dev.* 24, 1634–1644.
 46. Hua, Y., Vickers, T.A., Okunola, H.L., Bennett, C.F., and Krainer, A.R. (2008). Antisense masking of an hnRNP A1/A2 intronic splicing silencer corrects SMN2 splicing in transgenic mice. *Am. J. Hum. Genet.* 82, 834–848.
 47. Heo, Y.A. (2020). Golodirsen: first approval. *Drugs* 80, 329–333.
 48. Stein, C.A. (2016). Eteplirsen approved for Duchenne muscular dystrophy: the FDA faces a difficult choice. *Mol. Ther.* 24, 1884–1885.
 49. Summerton, J., and Weller, D. (1997). Morpholino antisense oligomers: design, preparation, and properties. *Antisense Nucleic Acid Drug Dev.* 7, 187–195.
 50. Wengel, J., Petersen, M., Nielsen, K.E., Jensen, G.A., Håkansson, A.E., Kumar, R., Sørensen, M.D., Rajwanshi, V.K., Bryld, T., and Jacobsen, J.P. (2001). LNA (locked nucleic acid) and the diastereoisomeric α -L-LNA: conformational tuning and high-affinity recognition of DNA/RNA targets. *Nucleosides Nucleotides Nucleic Acids* 20, 389–396.
 51. Kurreck, J., Wyszko, E., Gillen, C., and Erdmann, V.A. (2002). Design of antisense oligonucleotides stabilized by locked nucleic acids. *Nucleic Acids Res.* 30, 1911–1918.
 52. Castanotto, D., Lin, M., Kowolik, C., Wang, L., Ren, X.Q., Soifer, H.S., Koch, T., Hansen, B.R., Oerum, H., Armstrong, B., et al. (2015). A cytoplasmic pathway for gapmer antisense oligonucleotide-mediated gene silencing in mammalian cells. *Nucleic Acids Res.* 43, 9350–9361.
 53. Duschmalé, J., Hansen, H.F., Duschmalé, M., Koller, E., Albaek, N., Møller, M.R., Jensen, K., Koch, T., Wengel, J., and Bleicher, K. (2020). In vitro and in vivo properties of therapeutic oligonucleotides containing non-chiral 3' and 5' thiophosphate linkages. *Nucleic Acids Res.* 48, 63–74.
 54. Hagedorn, P.H., Persson, R., Funder, E.D., Albæk, N., Diemer, S.L., Hansen, D.J., Møller, M.R., Papargyri, N., Christiansen, H., Hansen, B.R., et al. (2018). Locked nucleic acid: modality, diversity, and drug discovery. *Drug Discov. Today* 23, 101–114.
 55. Yagui-Beltran, A., Craig, A.L., Lawrie, L., Thompson, D., Pospisilova, S., Johnston, D., Kernohan, N., Hopwood, D., Dillon, J.F., and Hupp, T.R. (2001). The human oesophageal squamous epithelium exhibits a novel type of heat shock protein response. *Eur. J. Biochem.* 268, 5343–5355.
 56. Imai, F.L., Uzawa, K., Nimura, Y., Moriya, T., Imai, M.A., Shiiba, M., Bukawa, H., Yokoe, H., and Tanzawa, H. (2005). Chromosome 1 open reading frame 10 (*C1orf10*) gene is frequently down-regulated and inhibits cell proliferation in oral squamous cell carcinoma. *Int. J. Biochem. Cell Biol.* 37, 1641–1655.
 57. Roblick, U.J., Bader, F.G., Hammarstedt, L., Habermann, J.K., Hellman, U., Becker, S., Sundmacker, A., Gemoll, T., Zimmermann, K., Auer, G., and Munck-Wikland, E. (2008). Proteomic analysis of protein expression in human tonsillar cancer: differentially expressed proteins characterize human tonsillar cancer. *Acta Oncol.* 47, 1493–1501.
 58. Kim, J.K., and Diehl, J.A. (2009). Nuclear cyclin D1: an oncogenic driver in human cancer. *J. Cell. Physiol.* 220, 292–296.
 59. Borgoño, C.A., and Diamandis, E.P. (2004). The emerging roles of human tissue kallikreins in cancer. *Nat. Rev. Cancer* 4, 876–890.
 60. Gnanapragasam, V.J., Robson, C.N., Neal, D.E., and Leung, H.Y. (2002). Regulation of FGF8 expression by the androgen receptor in human prostate cancer. *Oncogene* 21, 5069–5080.
 61. Gregory, C.W., Hamil, K.G., Kim, D., Hall, S.H., Pretlow, T.G., Mohler, J.L., and French, F.S. (1998). Androgen receptor expression in androgen-independent prostate cancer is associated with increased expression of androgen-regulated genes. *Cancer Res.* 58, 5718–5724.
 62. Xu, L.L., Shi, Y., Petrovics, G., Sun, C., Makarem, M., Zhang, W., Sesterhenn, I.A., McLeod, D.G., Sun, L., Moul, J.W., and Srivastava, S. (2003). PMEPA1, an androgen-regulated NEDD4-binding protein, exhibits cell growth inhibitory

- function and decreased expression during prostate cancer progression. *Cancer Res.* 63, 4299–4304.
63. Lin, B., Ferguson, C., White, J.T., Wang, S., Vessella, R., True, L.D., Hood, L., and Nelson, P.S. (1999). Prostate-localized and androgen-regulated expression of the membrane-bound serine protease *TMPRSS2*. *Cancer Res.* 59, 4180–4184.
64. Zhang, X., Castanotto, D., Liu, X., Shemi, A., and Stein, C.A. (2018). Ammonium and arsenic trioxide are potent facilitators of oligonucleotide function when delivered by gymnosin. *Nucleic Acids Res.* 46, 3612–3624.
65. Castanotto, D., Zhang, X., Alluin, J., Zhang, X., Rüger, J., Armstrong, B., Rossi, J., Riggs, A., and Stein, C.A. (2018). A stress-induced response complex (SIRC) shuttles miRNAs, siRNAs, and oligonucleotides to the nucleus. *Proc. Natl. Acad. Sci. USA* 115, E5756–E5765.
66. Hughes, C.S., Moggridge, S., Müller, T., Sorensen, P.H., Morin, G.B., and Krijgsveld, J. (2019). Single-pot, solid-phase-enhanced sample preparation for proteomics experiments. *Nat. Protoc.* 14, 68–85.
67. Perkins, D.N., Pappin, D.J., Creasy, D.M., and Cottrell, J.S. (1999). Probability-based protein identification by searching sequence databases using mass spectrometry data. *Electrophoresis* 20, 3551–3567.
68. Käll, L., Canterbury, J.D., Weston, J., Noble, W.S., and MacCoss, M.J. (2007). Semi-supervised learning for peptide identification from shotgun proteomics datasets. *Nat. Methods* 4, 923–925.
69. Welsh, E.A., Eschrich, S.A., Berglund, A.E., and Fenstermacher, D.A. (2013). Iterative rank-order normalization of gene expression microarray data. *BMC Bioinformatics* 14, 153.
70. Mellacheruvu, D., Wright, Z., Couzens, A.L., Lambert, J.P., St-Denis, N.A., Li, T., Miteva, Y.V., Hauri, S., Sardi, M.E., Low, T.Y., et al. (2013). The CRAPome: a contaminant repository for affinity purification-mass spectrometry data. *Nat. Methods* 10, 730–736.